Electronic Supplementary Material (ESI) for Physical Chemistry Chemical Physics.

Strain controlled electronic and magnetic properties in tVS$_2$/hVS$_2$ van der Waals heterostructures

Supporting Information

Dan Jin[+], [a] Meimei Shi[+], [a] Pan Li, [b] Huiyan Zhao,[a] Man Shen,[a] Fengxian Ma*, [b] Zhixue Tian*, [b] and Ying Liu [a]

[a] College of Physics, Hebei Advanced Thin Films Laboratory, Hebei Normal University, Shijiazhuang, 050024, China

[b] College of Physics, Hebei Key Laboratory of Photophysics Research and Application, Hebei Normal University, Shijiazhuang, 050024, China

[+] These authors contributed equally to this work.

* To whom correspondence should be addressed.

Tel: 86-311-80787350

E-mail: fengxianma@hebtu.edu.cn

E-mail: zxtian@hebtu.edu.cn

Table S1. Total energies and the interface formation energies of these six possible configurations (without rotation) calculated using a 20×20×1 and a 15×15×1 *k*-mesh, respectively. The red data were obtained from the 15×15×1 *k*-mesh calculations. The total energies of the H-phase and the T-phase of the VS_2 monolayers, and their bilayers calculated by PBE with (w-vdW) and without (wo-vdW) the vdW correction were also listed here. The interface formation energies were calculated based on Eq. (1) and Eq. (2).

Total energy (eV)		mono. wo-vdW		mono. w-vdW		bilayer w-vdW	
		T: -19.7133	H: -19.7527	T: -20.1822	H: -20.2016	T: -40.5140	H: -40.5468
top-I	-40.4795	-0.169		-0.016		0.0084	
	-40.4798						
top-II	-40.4803	-0.169		-0.016		0.0084	
	-40.4806						
hcp-I	-40.5253	-0.177		-0.024		0.0008	
	-40.5255						
hcp-II	-40.5278	-0.177		-0.024		0.0004	
	-40.5280						
fcc-I	-40.5370	-0.179		-0.026		-0.0011	
	-40.5372						
fcc-II	-40.5382	-0.179		-0.026		-0.0013	
	-40.5385						

Fig. S1. (a) The density of states of the *fcc*-I heterostructure respect to the GGA + U method. (b) The band structure of the *fcc*-II configuration calculated by GGA + U. (c) The FM, NM, and AFM configurations of the *fcc*-II heterostructure. Here "E" represents the energy difference with respect to the FM state, which were obtained in the PBE calculations. (d) The spin densities of the *fcc*-II tVS$_2$/hVS$_2$ heterostructure.

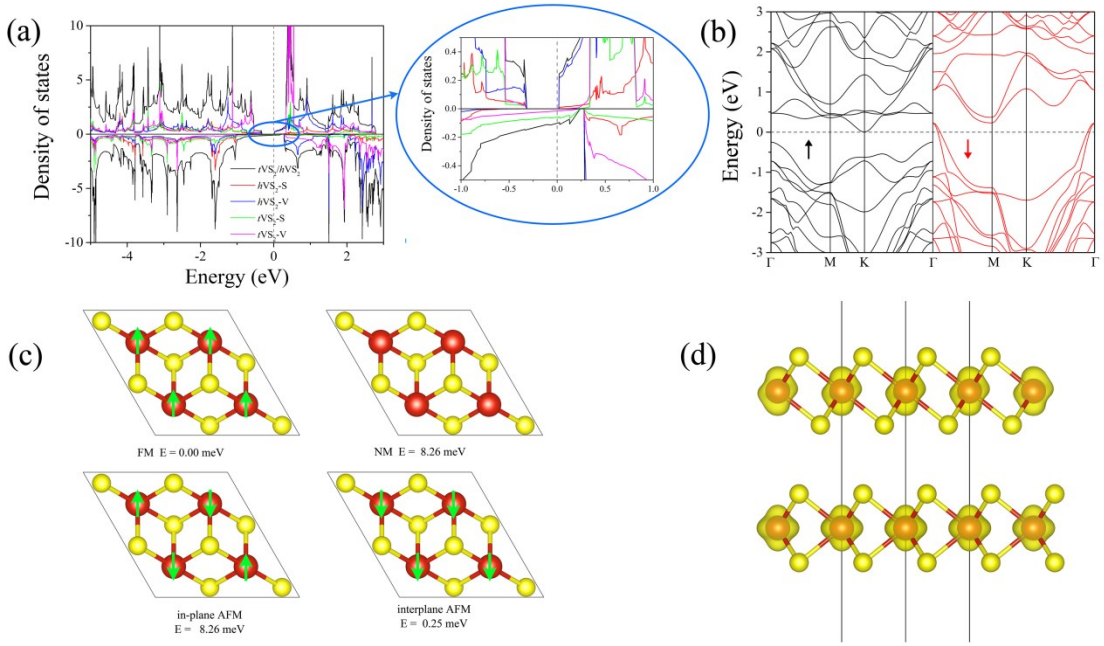

Fig. S2. (a) The FM, inter-AFM, and inplane-AFM states of the *fcc*-I configuration in a (4×4×1) supercell. "E" represents the energy difference with respect to the FM state. All energies were obtained in the PBE calculations. (b) and (c) are for the dependence of the energy per unit cell on the strain for the FM and AFM states of the tVS$_2$/hVS$_2$ heterostructure with the *fcc*-I and *fcc*-II configurations, respectively.

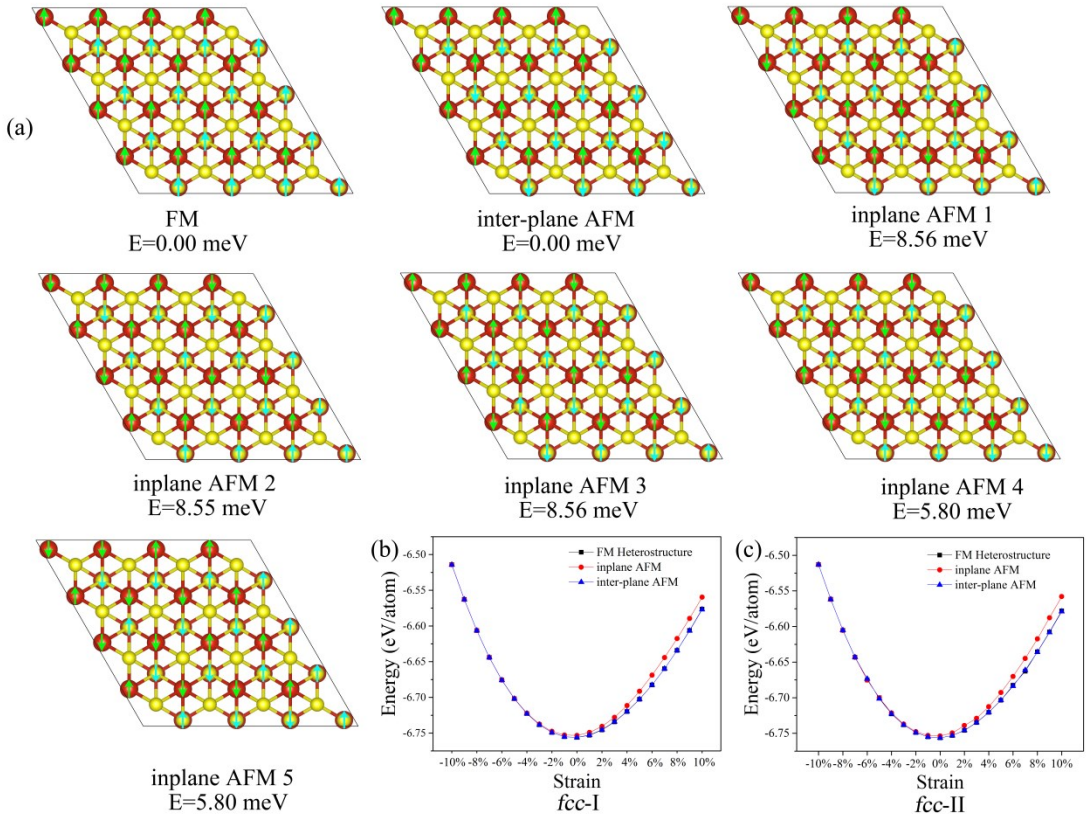

Fig. S3. Orbital decomposed band structures of the FM *t*VS_2/*h*VS_2 heterostructure calculated by GGA+U method. (a) and (b) are for the spin-up and spin-down states, respectively.

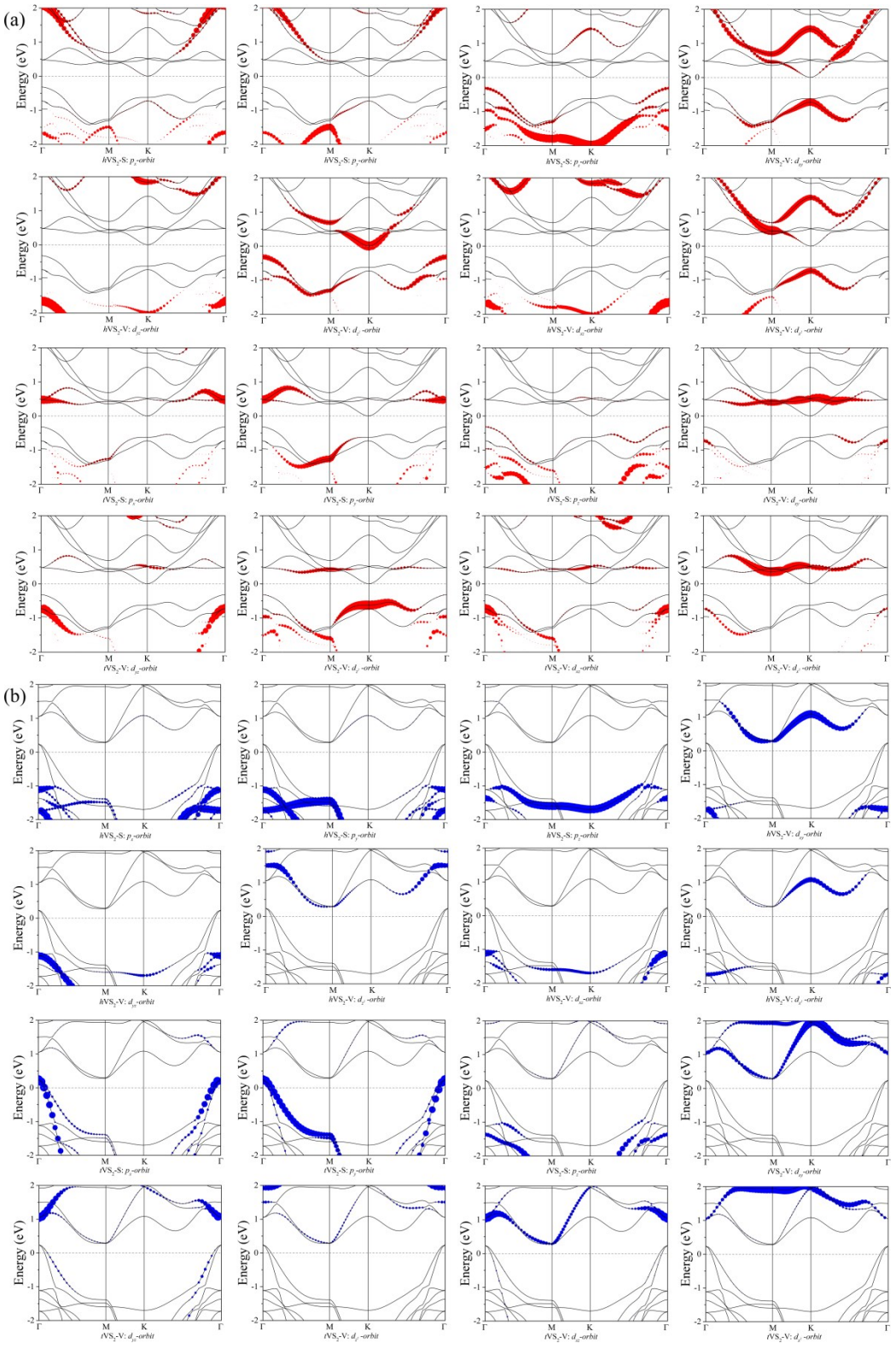

Fig. S4. Electronic band structures of the AFM *t*VS_2/*h*VS_2 heterostructures using different methods.

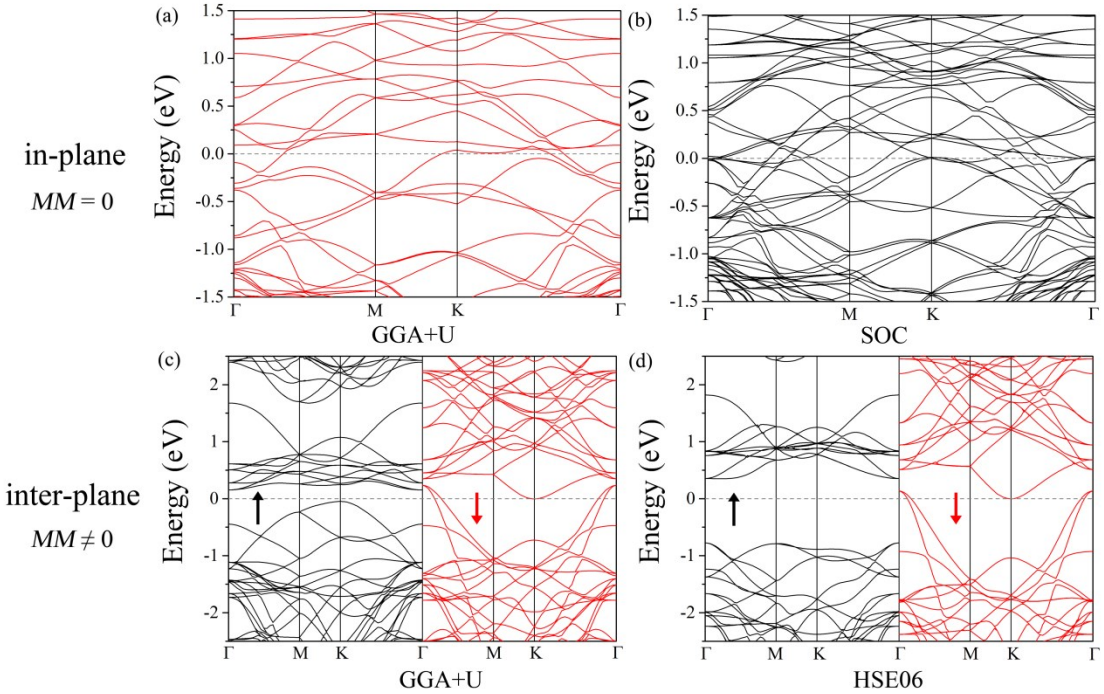

Fig. S5. The band structures of the tVS$_2$/hVS$_2$ heterostructures with biaxial (a) compressive strains from 1%~10% and (b) tensile strains from 1%~10%.

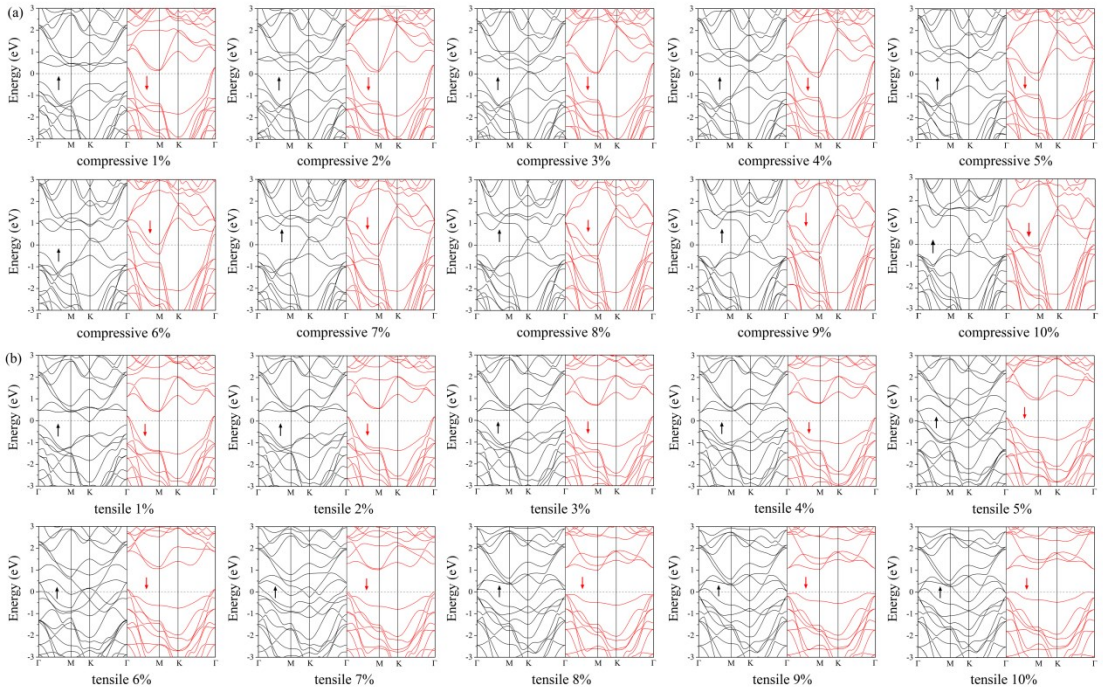

Fig. S6. Interlayer distance of tVS$_2$/hVS$_2$ heterostructure with different strains.

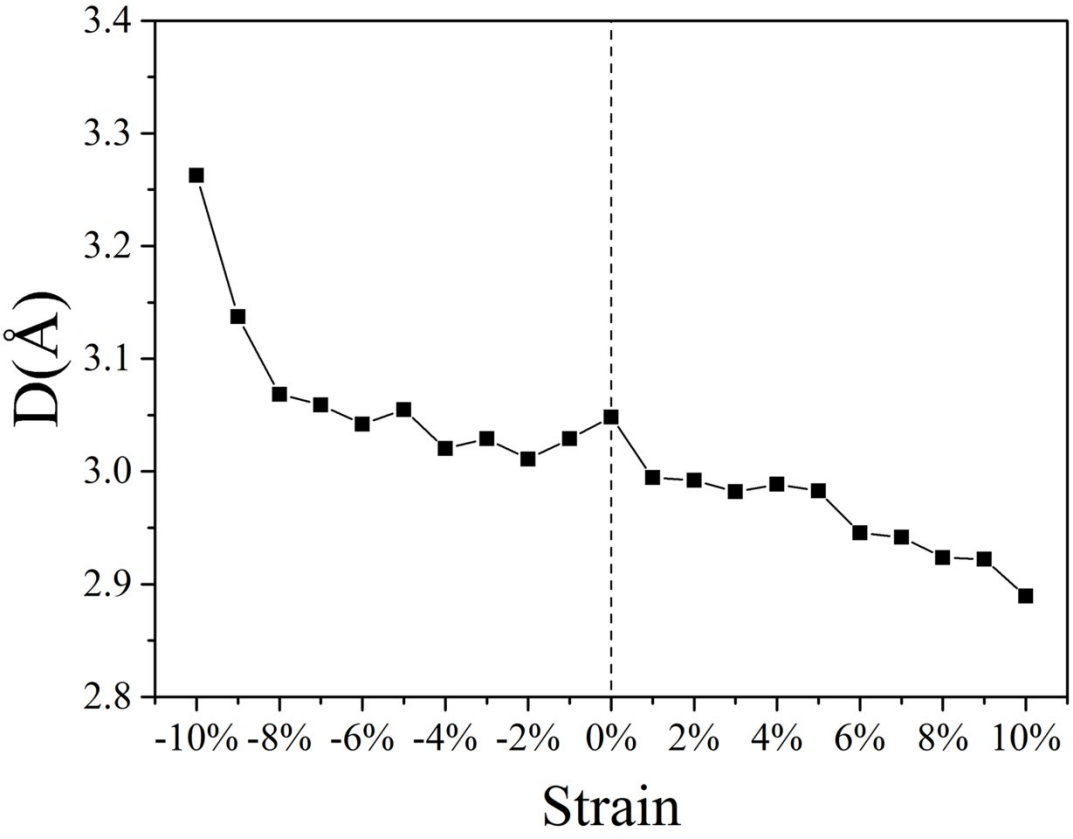

Fig. S7. Orbital decomposed band structures of tVS$_2$/hVS$_2$ heterostructure with a tensile strain of 5%, (a) and (b) are for the spin-up and spin-down states, respectively.